nature medicine

Slitrk5 deficiency impairs corticostriatal circuitry and leads to obsessive-compulsive–like behaviors in mice

Sergey V Shmelkov[1,9], Adília Hormigo[1–3,9], Deqiang Jing[4,9], Catia C Proenca[4,5,9], Kevin G Bath[4], Till Milde[1], Evgeny Shmelkov[1], Jared S Kushner[1], Muhamed Baljevic[1], Iva Dincheva[4,6], Andrew J Murphy[7], David M Valenzuela[7], Nicholas W Gale[7], George D Yancopoulos[7], Ipe Ninan[8], Francis S Lee[4,6] & Shahin Rafii[1]

Obsessive-compulsive disorder (OCD) is a common psychiatric disorder defined by the presence of obsessive thoughts and repetitive compulsive actions, and it often encompasses anxiety and depressive symptoms[1,2]. Recently, the corticostriatal circuitry has been implicated in the pathogenesis of OCD[3,4]. However, the etiology, pathophysiology and molecular basis of OCD remain unknown. Several studies indicate that the pathogenesis of OCD has a genetic component[5–8]. Here we demonstrate that loss of a neuron-specific transmembrane protein, SLIT and NTRK-like protein-5 (Slitrk5), leads to OCD-like behaviors in mice, which manifests as excessive self-grooming and increased anxiety-like behaviors, and is alleviated by the selective serotonin reuptake inhibitor fluoxetine. *Slitrk5*$^{-/-}$ mice show selective overactivation of the orbitofrontal cortex, abnormalities in striatal anatomy and cell morphology and alterations in glutamate receptor composition, which contribute to deficient corticostriatal neurotransmission. Thus, our studies identify Slitrk5 as an essential molecule at corticostriatal synapses and provide a new mouse model of OCD-like behaviors.

There are several disorders that have OCD-like clinical manifestations[9], such as obsessive-compulsive disorder, Gilles de la Tourette's syndrome and trichotillomania. Recent human genetic analyses have linked the *SLITRK1* gene to Tourette's syndrome[10], although the underlying mechanisms are not well understood. The *Slitrk1* gene belongs to a new family of six members (*Slitrk1*–*Slitrk6*) encoding one-pass transmembrane proteins that contain two extracellular leucine-rich repeat domains, similar to Slit proteins, and a carboxy-terminal domain that is similar to Trk neurotrophin receptors. These proteins have been shown to affect neuronal process outgrowth[11,12]. *Slitrk1*-knockout mice show increased anxiety-like behaviors but do not show any other behavioral abnormalities[13]. Although little is known about Slitrk1, the function of other members of the Slitrk family remains even more obscure. By gene expression fingerprinting, we have previously identified *Slitrk5* in hematopoietic progenitors[14]. Subsequently, we demonstrated that human SLITRK5 is expressed in leukemias, embryonic stem cells and subsets of endothelial cells[15]. However, the *Slitrk5* gene is expressed predominantly in neural tissues[12].

We hypothesized that abnormal expression of Slitrk5 may lead to behavioral phenotypes similar to the involvement of SLITRK1 in Tourette's syndrome. To investigate the function of this protein and to delineate the expression pattern of the *Slitrk5* gene in mouse tissues, we decided to create a knockout mouse by replacing the *Slitrk5* gene with a reporter gene. Analysis of the genomic structure of the *Slitrk5* gene revealed that the coding region is localized to a single exon. Using Velocigene technology[16], we replaced the entire encoding exon with the *lacZ* gene (**Fig. 1a**). Expression analysis of *lacZ* showed that *Slitrk5* is widely expressed throughout the central nervous system, including the cortex and striatum (**Fig. 1b**). Double staining for the neuronal marker NeuN showed that in the brain *Slitrk5* expression is restricted to neurons and that the majority of neurons express *Slitrk5* (**Fig. 1c**).

Slitrk5$^{-/-}$ mice were born in accordance with Mendelian distribution. Gross anatomical and thorough histological examination of young *Slitrk5*$^{-/-}$ mice did not show any abnormalities. However, analysis of older *Slitrk5*$^{-/-}$ mice revealed a behavioral phenotype. Starting at 3 months of age, *Slitrk5*$^{-/-}$ mice developed facial hair loss and severe skin lesions. Over time, these lesions produced ulcerations with hemorrhage (**Fig. 2a**). The penetrance of this phenotype increased with age, and most of the knockout as well as the heterozygous mice were affected. The lesions in heterozygous mice were similar to those in homozygous mice, but their emergence was delayed by 7–9 months. We hypothesized that this phenotype could be the result of excessive grooming. We did not find the lesions in the wild-type littermates, even when they were housed in the same cage with *Slitrk5*$^{-/-}$ mice, indicating that this phenotype can be attributed to self-grooming. This type of behavior is similar to that previously observed in mice deficient for the *Sapap3* gene[17]. Targeted deletion of this gene, which encodes a postsynaptic scaffold protein, leads to compulsive

[1]Howard Hughes Medical Institute, Ansary Stem Cell Institute and Department of Genetic Medicine, Weill Cornell Medical College, New York, New York, USA. [2]Department of Neurology, Memorial Sloan-Kettering Cancer Center, New York, New York, USA. [3]Department of Neurology, Weill Cornell Medical College, New York, New York, USA. [4]Department of Psychiatry, Weill Cornell Medical College, New York, New York, USA. [5]Gulbenkian PhD Programe in Biomedicine, Instituto Gulbenkian de Ciência, Oeiras, Portugal. [6]Department of Pharmacology, Weill Cornell Medical College, New York, New York, USA. [7]Regeneron Pharmaceuticals, Tarrytown, New York, USA. [8]Department of Psychiatry, New York University Langone Medical Center, New York, New York, USA. [9]These authors contributed equally to this work. Correspondence should be addressed to F.S.L. (fslee@med.cornell.edu) or S.R. (srafii@med.cornell.edu).

Received 29 October 2009; accepted 22 February 2010; published online 25 April 2010; doi:10.1038/nm.2125

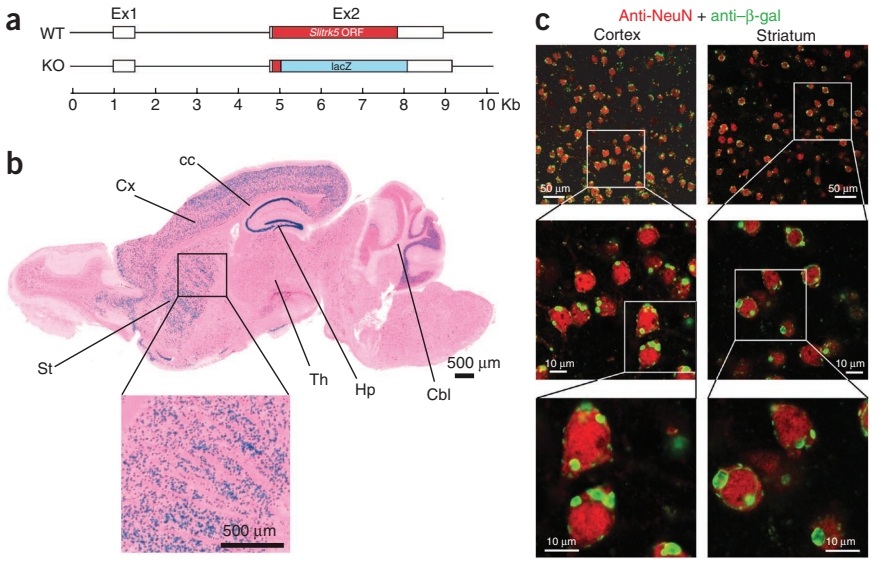

Figure 1 Targeted inactivation of Slitrk5 in mice and its expression pattern in the mouse brain. (**a**) Genomic structure and the design of the *Slitrk5*-knockout, *lacZ*–knock-in mouse. The entire open reading frame (ORF) is localized to exon 2 (Ex2); exon 1 (Ex1) is noncoding. The *Slitrk5*-encoding region was replaced with *lacZ* downstream of the signal sequence cleavage site. WT, wild-type; KO, knockout. (**b**) X-gal staining of mouse brain tissue, showing ubiquitous expression of lacZ in the gray matter of the various parts of the brain, including cortex and striatum. Cx, cortex; St, striatum; Hp, hippocampus; cc, corpus callosum; Th, thalamus; Cbl, cerebellum. The higher magnification image shows the distribution of *lacZ*-expressing cells in the striatum of the *Slitrk5*-knockout, *lacZ*–knock-in mouse. (**c**) Immunostaining of cortex and striatum with antibodies to β-galactosidase (anti–β-gal) and NeuN (anti-NeuN), indicating that the majority of neurons express *Slitrk5*.

overgrooming behavior and increased anxiety, which are ameliorated by selective serotonin reuptake inhibitors[17].

We assessed the grooming behavior of *Slitrk5*$^{-/-}$ mice by counting the number and duration of grooming events in the knockout and wild-type littermates before any lesions or hair loss developed to exclude the possibility that the overgrooming was due to irritation in a wound area. Our data show a significant increase in the duration of grooming events in *Slitrk5*$^{-/-}$ mice as compared to their wild-type littermates (**Fig. 2b**).

As OCD is linked to a deficit in serotonin production, and because selective serotonin reuptake inhibitors (SSRIs) are the major therapeutic agents for OCD, we sought to test the effect of chronic administration of the SSRI fluoxetine on overgrooming behavior in *Slitrk5*$^{-/-}$ mice. Indeed, treatment of *Slitrk5*$^{-/-}$ mice with fluoxetine led to a significant ($P = 0.0009$) reduction in the duration of grooming compared to pretreated mice (**Fig. 2b**). The duration of grooming in *Slitrk5*$^{-/-}$ mice after fluoxetine treatment was the same as in wild-type littermates (**Fig. 2b**). The duration of grooming events in wild-type mice was not affected by fluoxetine (**Fig. 2b**). Thus, treatment of *Slitrk5*$^{-/-}$ mice with an SSRI prevents their compulsive behavior.

To determine whether *Slitrk5*$^{-/-}$ mice show additional behavioral phenotypes that also occur in OCD-related conditions, we assessed anxiety-like behaviors in these mice. We performed the elevated-plus-maze and the open-field tests, standard measures of anxiety-like behavior that place the mice in conflict situations. In comparison with wild-type littermate mice, *Slitrk5*$^{-/-}$ mice showed a lower percentage of time spent in the center compartment and a lower number of entries into the center compartment in the open-field test (**Fig. 2c**), and they showed reduced time spent in open arms in the elevated-plus-maze test (**Supplementary Fig. 1a**). This reduction in exploration could not be explained by changes in locomotor activity, as there were no significant differences in total distance traveled. To further assess the behavioral consequences of Slitrk5 inactivation, we also tested *Slitrk5*$^{-/-}$ mice in a marble-burying paradigm, a behavioral task that assesses both OCD-like and anxiety-related behaviors. We found that *Slitrk5*$^{-/-}$ mice showed an increase in marble-burying behavior (**Supplementary Fig. 1b**), which is consistent with our findings that this knockout mouse models core symptoms in OCD spectrum disorders. We also assessed motor function in *Slitrk5*$^{-/-}$ mice by using the cylinder test and by measuring the latency to fall from a rotarod and found no difference in gross motor skills and no impairment in motor learning compared to wild-type mice, indicating that these functions are not affected in *Slitrk5*$^{-/-}$ mice (**Supplementary Fig. 2** and **Supplementary Fig. 3**).

Because corticostriatal circuitry has been previously implicated in the pathogenesis of OCD, we performed detailed anatomical, histological and functional analyses of cortex and striatum in *Slitrk5*$^{-/-}$ mice. Initially, we evaluated the difference in baseline activity of selected brain regions between wild-type and *Slitrk5*$^{-/-}$ mice by assessing expression of FosB, an established marker for neural activity[18]. We found that FosB was upregulated exclusively in the orbitofrontal cortex of *Slitrk5*$^{-/-}$ mice (**Fig. 3a**,**b**). Other brain regions such as the caudate putamen, hippocampus and thalamus did not show upregulation of FosB expression (**Supplementary Fig. 4**). These findings are particularly noteworthy, as it has been consistently shown in functional imaging studies that there is an increase in orbitofrontal cortex activity in individuals with OCD[4,19–21]. Conversely, alterations in neural

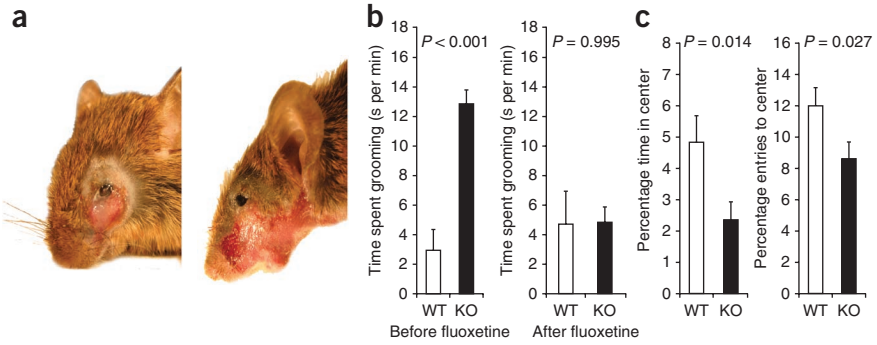

Figure 2 Facial lesions, OCD-like behavior and its alleviation with fluoxetine treatment in *Slitrk5*-knockout mice. (**a**) Phenotypic characteristic of *Slitrk5*$^{-/-}$ mice: excessive grooming leads to severe facial lesions. (**b**) Time spent grooming in *Slitrk5*$^{-/-}$ mice ($n = 9$) compared to their wild-type littermates ($n = 8$) before and after treatment with fluoxetine. Error bars depict the s.e.m. (**c**) Anxiety-related behavior of *Slitrk5*$^{-/-}$ and WT mice in the open-field test. Percentage of time spent in the center and entries into the center of the open field are shown. All open-field results are presented as means ± s.e.m. determined from analysis of 20 mice per genotype.

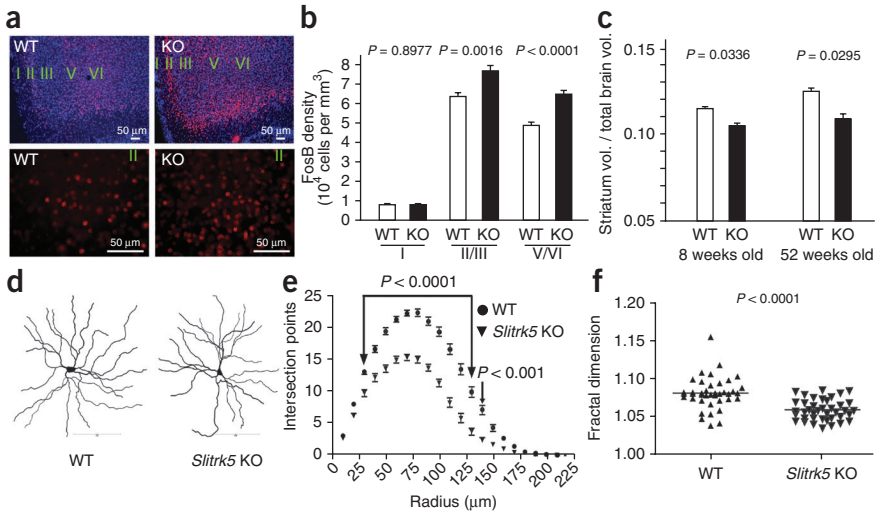

Figure 3 Metabolic changes in the cortex and anatomical defects in the striatum of *Slitrk5*$^{-/-}$ mice. (**a**) Expression of FosB in orbitofrontal cortex by immunostaining for FosB (red) and with DAPI (blue). The top images show the distribution of FosB expression in the various layers of orbitofrontal cortex. The bottom images show a higher magnification of layer II of FosB immunoreactivity in nuclei. (**b**) Quantification of FosB expression in all layers of the orbitofrontal cortex. (**c**) Cavalieri estimation of striatal volume in *Slitrk5*$^{-/-}$ and WT mice. (**d**) Examples of Golgi staining and Neurolucida reconstruction of striatal medium spiny neurons in WT and *Slitrk5*$^{-/-}$ mice. (**e**) Sholl analysis of striatal medium spiny neurons in WT and *Slitrk5*$^{-/-}$ mice. All results are presented as means ± s.e.m.; 40 neurons per genotype. (**f**) Fractal dimension analysis of striatal medium spiny neurons in *Slitrk5*$^{-/-}$ and WT mice. All results are presented as means ± s.e.m.; 40 neurons per genotype.

activity in the caudate or thalamus have been less consistently found in OCD[19,21,22]. Next, we measured the volume of the striatum relative to the whole-brain volume by Cavalieri estimation. Our data showed that the volume of striatum in *Slitrk5*$^{-/-}$ mice was significantly reduced compared to wild-type mice (**Fig. 3c**). In both young and aged *Slitrk5*$^{-/-}$ mice, the ratio of striatal volume to the total brain volume was decreased compared to wild-type mice, whereas volume ratios of other brain structures, such as the dorsal hippocampus, to the total brain volume were not changed, indicating that the anatomy of striatum is specifically affected by Slitrk5 deficiency (**Fig. 3c** and **Supplementary Fig. 5**). In line with these data, it has previously been reported that the volume of the striatum is decreased in some individuals with OCD[23–25]. However, this finding has not been consistent across all studies of individuals with OCD in which increased or no change in striatal volumes have been reported[19,21,22].

Because Slitrk family members have been shown to influence neuronal differentiation[10,12], the decreased striatal volume in the *Slitrk5*$^{-/-}$ mice might be accounted for by altered neuronal morphology. We used Golgi staining to visualize individual medium spiny neurons of the striatum in *Slitrk5*$^{-/-}$ mice. There was no difference in striatal cell soma area between *Slitrk5*$^{-/-}$ mice and their wild-type littermates. Next, we analyzed dendritic complexity in the same neurons. Sholl analysis revealed a decrease in dendritic arbor complexity at 50-µm and greater distances from the soma in *Slitrk5*$^{-/-}$ mice (**Fig. 3d**,**e**). We also used fractal dimension analysis to quantify how completely a neuron fills its dendritic field. There was a significant decrease in dendritic complexity of striatal neurons in *Slitrk5*$^{-/-}$ mice (**Fig. 3f**). Although the striatum contains two equally abundant subpopulations of medium spiny neurons, which are classified on the basis of the neuropeptides that they produce and the dopamine receptors that they express (D_1 and D_2), distinguishing between these two types of cells is technically challenging[26]. However, in our detailed comparative analysis of 40 randomly selected medium spiny neurons in *Slitrk5*$^{-/-}$ mice, we found no evidence for a bimodal distribution in their dendritic complexity (**Fig. 3e**,**f**). These data suggest that there is no selective deficit of arborization in one subpopulation of medium spiny neurons but rather a general deficit in all medium spiny neurons. Sholl and fractal dimension analyses of neurons in other brain regions with high Slitrk5 expression such as dentate granular cells showed no difference in dendritic branching complexity (**Supplementary Fig. 6**).

We subsequently assessed the cellular localization of Slitrk5 in striatal neurons and found Slitrk5 in dendritic spines that are positive for postsynaptic density protein-95 (PSD95) in cocultures of cortical neurons, isolated from transgenic mice that express enhanced GFP under the control of the human ubiquitin C promoter, and rat striatal neurons infected with Flag-Slitrk5 lentivirus and transfected with PSD95 fused to mCherry (**Fig. 4a**). Next, we examined the expression of glutamate receptors in

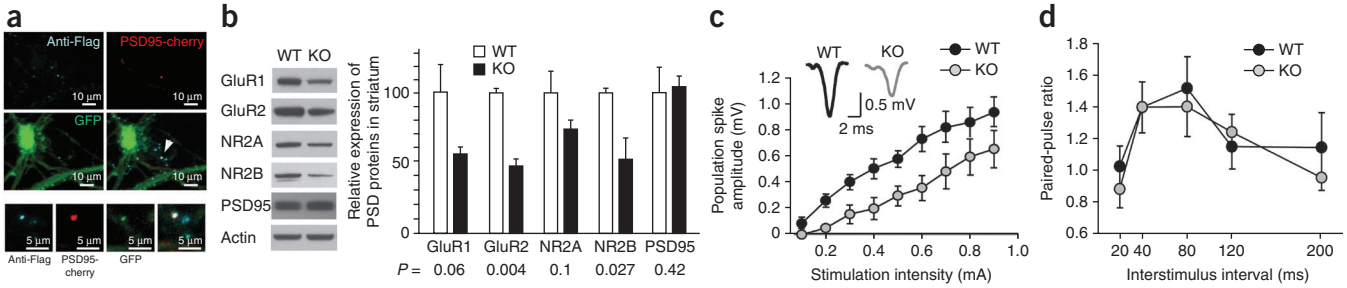

Figure 4 Deficiency in corticostriatal transmission in *Slitrk5*$^{-/-}$ mice is mediated by changes in glutamate receptor composition. (**a**) Immunostaining of primary striatal rat neurons (infected with Flag-Slitrk5 lentivirus and transfected with PSD95 fused to mCherry (PSD95-cherry)) in culture with cortical neurons (isolated from transgenic mice that ubiquitously express green fluorescent protein) with Flag-specific antibody (anti-Flag). The arrow points to a magnified area (bottom images) that represents the synapses between cortical and striatal neurons. (**b**) Western blot analysis of NMDA and AMPA receptor subunits in the striatum of 5-month-old *Slitrk5*$^{-/-}$ and WT mice. The protein amounts are adjusted to the expression of actin. (**c**) Population spike amplitude in *Slitrk5*$^{-/-}$ mice ($n = 11$, from four mice) and matched WT mice ($n = 9$, from four mice). The population spike amplitude is significantly lower in *Slitrk5*$^{-/-}$ mice, $P < 0.01$, repeated-measures analysis of variance. The inset shows examples of corticostriatal population spike amplitudes in *Slitrk5*$^{-/-}$ mice and matched WT mice. (**d**) Average paired-pulse ratios of the population spike in *Slitrk5*$^{-/-}$ mice ($n = 17$, from five mice) and matched WT mice ($n = 17$, from five mice). There is no significant difference in the paired-pulse ratio between *Slitrk5*$^{-/-}$ mice and wild-type mice.

the striatum and found that they are downregulated in *Slitrk5*$^{-/-}$ mice (**Fig. 4b**). Indeed, protein amounts of glutamate receptor subunits NR2A, NR2B, GluR1, and GluR2 were decreased by 20–60%, with no significant changes in PSD95 amounts (**Fig. 4b**). We found these changes in both the total lysates (**Fig. 4b**) and in PSD-enriched fractions of synaptosomes (**Supplementary Fig. 7**).

Given these findings, we investigated whether *Slitrk5*$^{-/-}$ mice have deficits in corticostriatal neurotransmission by extracellular recordings in acute striatal slices. We recorded population spikes from striatum by stimulating the white matter between cortex and striatum. We found a significantly reduced population spike amplitude in *Slitrk5*$^{-/-}$ mice (**Fig. 4c**). We did not observe any difference in paired-pulse ratios of the population spike in *Slitrk5*$^{-/-}$ mice and their wild-type littermates, suggesting that the presynaptic mechanism involved in paired-pulse facilitation is not responsible for the observed difference in population spike amplitude (**Fig. 4d**). Also, we did not observe any significant difference in fiber volley amplitude, suggesting that cortical axon input is normal in *Slitrk5*$^{-/-}$ mice (**Supplementary Fig. 8**).

Taken together, our data demonstrate that targeted inactivation of *Slitrk5* in mice leads to OCD-like behavioral phenotypes, including overgrooming with elements of self-mutilation. Although Slitrk5 expression is widespread in the central nervous system, we found increased neuronal activity specifically in the orbitofrontal cortex of *Slitrk5*$^{-/-}$ mice, which is consistent with functional imaging findings in humans with OCD that implicated dysregulation of corticostriatal circuitry[23,27], and which has not been reported in previous mouse models of OCD[28,29]. In addition, *Slitrk5*$^{-/-}$ mice have anatomical deficits in the striatum, such as reduced striatal volume, as well as decreased dendritic complexity of striatal medium spiny neurons. Although this region has not been consistently found to be altered anatomically in people with OCD[19,21,22], emerging literature suggests that striatal dysfunction may underlie behavioral deficits in individuals with OCD[27]. In this context, it has recently been postulated that striatal dysfunction, in the presence of orbitofrontal cortex overactivation, could lead to deficits in thalamic filtering or imbalance in the direct and indirect pathways of the basal ganglia[30]. Given the ubiquitous neuronal expression of Slitrk5, this selective effect on the orbitofrontal cortex and on striatal neurons is hard to explain. On the one hand, it is reminiscent of the effect of other proteins such as huntingtin, which is also widely expressed in the central nervous system, but alterations in the huntingtin protein result in functional defects predominantly in striatal neurons, directly leading to Huntington's disease pathology[31]. On the other hand, it is possible that Slitrk5 may form a signaling complex with corticostriatal-specific proteins, which may explain these region-specific effects.

Overall, our data suggest that Slitrk5 may have a central role in the development of OCD-like behaviors. Although human genetic studies have implicated another Slitrk family member, SLITRK1, in Tourette's syndrome, these associations have not been consistently replicated[32,33]. In this context, our studies link Slitrk5 to the core symptoms of OCD: self-injurious repetitive behavior and increased anxiety. In all, we provide a new mouse model of OCD-like behaviors, involving a previously uncharacterized neuronal transmembrane protein that modulates region-specific glutamatergic neurotransmission. This model can be used to further dissect the role of Slitrk5 in molecular pathways underlying the pathogenesis of obsessive-compulsive behaviors.

METHODS

Methods and any associated references are available in the online version of the paper at http://www.nature.com/naturemedicine/.

Note: Supplementary information is available on the Nature Medicine website.

ACKNOWLEDGMENTS

We thank M. Flint Beal for providing expertise on behavioral experiments. We thank G. Thurston for critical comments and suggestions. PSD95-cherry was a kind gift from R.H. Edwards (University of California–San Francisco). We acknowledge support from US National Institutes of Health grants MH079513 (F.S.L.) and NS052819 (F.S.L.), HL66592 (S.R.), HL097797 (S.R.) and AI080309 (S.R.), Burroughs Wellcome Foundation (F.S.L.), International Mental Health Research Organization (F.S.L.), the Sackler Institute (K.G.B., F.S.L.), DeWitt-Wallace Fund of the New York Community Trust (F.S.L.), Pritzker Consortium (F.S.L.), National Alliance for Research on Schizophrenia and Depression (S.V.S.), Mildred-Scheel-Stiftung, Deutsche Krebshilfe (T.M.), Gulbenkian PhD Programe in Biomedicine (C.C.P.), Fundacao para Ciencia e Tecnologia (C.C.P.), Howard Hughes Medical Institute (S.R.), Ansary Stem Cell Institute (S.R.), Anbinder and Newmans Own Foundations (S.R.), Qatar National Priorities Research Program (S.R.), Empire State Stem Cell Board (S.R.) and the New York State Department of Health grant NYS C024180 (S.R.).

AUTHOR CONTRIBUTIONS

S.V.S. conceived of and designed the study, performed experiments, analyzed data and wrote the manuscript; A.H., D.J, C.C.P. and K.G.B. designed and performed experiments, analyzed data and assisted in writing the manuscript; T.M., E.S., J.S.K., M.B. and I.D. performed experiments and analyzed data; A.J.M., D.M.V., N.W.G. and G.D.Y. designed and generated the *Slitrk5*$^{-/-}$ mice; I.N. designed, performed and analyzed electrophysiology experiments; F.S.L. and S.R. conceived of and designed the study and wrote the manuscript.

COMPETING FINANCIAL INTERESTS

The authors declare no competing financial interests.

Published online at http://www.nature.com/naturemedicine/.
Reprints and permissions information is available online at http://npg.nature.com/reprintsandpermissions/.

1. Miguel, E.C. *et al.* Obsessive-compulsive disorder phenotypes: implications for genetic studies. *Mol. Psychiatry* **10**, 258–275 (2005).
2. Karno, M., Golding, J.M., Sorenson, S.B. & Burnam, M.A. The epidemiology of obsessive-compulsive disorder in five US communities. *Arch. Gen. Psychiatry* **45**, 1094–1099 (1988).
3. Graybiel, A.M. & Rauch, S.L. Toward a neurobiology of obsessive-compulsive disorder. *Neuron* **28**, 343–347 (2000).
4. Menzies, L. *et al.* Integrating evidence from neuroimaging and neuropsychological studies of obsessive-compulsive disorder: the orbitofronto-striatal model revisited. *Neurosci. Biobehav. Rev.* **32**, 525–549 (2008).
5. Clifford, C.A., Murray, R.M. & Fulker, D.W. Genetic and environmental influences on obsessional traits and symptoms. *Psychol. Med.* **14**, 791–800 (1984).
6. Rasmussen, S.A. & Tsuang, M.T. The epidemiology of obsessive compulsive disorder. *J. Clin. Psychiatry* **45**, 450–457 (1984).
7. Pauls, D.L., Alsobrook, J.P. II, Goodman, W., Rasmussen, S. & Leckman, J.F. A family study of obsessive-compulsive disorder. *Am. J. Psychiatry* **152**, 76–84 (1995).
8. Nestadt, G. *et al.* A family study of obsessive-compulsive disorder. *Arch. Gen. Psychiatry* **57**, 358–363 (2000).
9. Hollander, E., Kim, S., Khanna, S. & Pallanti, S. Obsessive-compulsive disorder and obsessive-compulsive spectrum disorders: diagnostic and dimensional issues. *CNS Spectr.* **12**, 5–13 (2007).
10. Abelson, J.F. *et al.* Sequence variants in SLITRK1 are associated with Tourette's syndrome. *Science* **310**, 317–320 (2005).
11. Aruga, J. & Mikoshiba, K. Identification and characterization of Slitrk, a novel neuronal transmembrane protein family controlling neurite outgrowth. *Mol. Cell. Neurosci.* **24**, 117–129 (2003).
12. Aruga, J., Yokota, N. & Mikoshiba, K. Human SLITRK family genes: genomic organization and expression profiling in normal brain and brain tumor tissue. *Gene* **315**, 87–94 (2003).
13. Katayama, K. *et al.* Slitrk1-deficient mice display elevated anxiety-like behavior and noradrenergic abnormalities. *Mol. Psychiatry* **15**, 177–184 (2010).
14. Shmelkov, S.V., Visser, J.W. & Belyavsky, A.V. Two-dimensional gene expression fingerprinting. *Anal. Biochem.* **290**, 26–35 (2001).
15. Milde, T. *et al.* A novel family of slitrk genes is expressed on hematopoietic stem cells and leukemias. *Leukemia* **21**, 824–827 (2007).
16. Valenzuela, D.M. *et al.* High-throughput engineering of the mouse genome coupled with high-resolution expression analysis. *Nat. Biotechnol.* **21**, 652–659 (2003).
17. Welch, J.M. *et al.* Cortico-striatal synaptic defects and OCD-like behaviours in Sapap3-mutant mice. *Nature* **448**, 894–900 (2007).
18. McClung, C.A. *et al.* DeltaFosB: a molecular switch for long-term adaptation in the brain. *Brain Res. Mol. Brain Res.* **132**, 146–154 (2004).
19. Saxena, S., Bota, R.G. & Brody, A.L. Brain-behavior relationships in obsessive-compulsive disorder. *Semin. Clin. Neuropsychiatry* **6**, 82–101 (2001).

20. Whiteside, S.P., Port, J.D. & Abramowitz, J.S. A meta-analysis of functional neuroimaging in obsessive-compulsive disorder. *Psychiatry Res.* **132**, 69–79 (2004).
21. Saxena, S. & Rauch, S.L. Functional neuroimaging and the neuroanatomy of obsessive-compulsive disorder. *Psychiatr. Clin. North Am.* **23**, 563–586 (2000).
22. Aylward, E.H. *et al.* Normal caudate nucleus in obsessive-compulsive disorder assessed by quantitative neuroimaging. *Arch. Gen. Psychiatry* **53**, 577–584 (1996).
23. Robinson, D. *et al.* Reduced caudate nucleus volume in obsessive-compulsive disorder. *Arch. Gen. Psychiatry* **52**, 393–398 (1995).
24. Rosenberg, D.R. *et al.* Frontostriatal measurement in treatment-naive children with obsessive-compulsive disorder. *Arch. Gen. Psychiatry* **54**, 824–830 (1997).
25. Szeszko, P.R. *et al.* Brain structural abnormalities in psychotropic drug-naive pediatric patients with obsessive-compulsive disorder. *Am. J. Psychiatry* **161**, 1049–1056 (2004).
26. Surmeier, D.J., Ding, J., Day, M., Wang, Z. & Shen, W. D1 and D2 dopamine-receptor modulation of striatal glutamatergic signaling in striatal medium spiny neurons. *Trends Neurosci.* **30**, 228–235 (2007).
27. Rauch, S.L. *et al.* Functional magnetic resonance imaging study of regional brain activation during implicit sequence learning in obsessive-compulsive disorder. *Biol. Psychiatry* **61**, 330–336 (2007).
28. Wang, L., Simpson, H.B. & Dulawa, S.C. Assessing the validity of current mouse genetic models of obsessive-compulsive disorder. *Behav. Pharmacol.* **20**, 119–133 (2009).
29. Joel, D. Current animal models of obsessive compulsive disorder: a critical review. *Prog. Neuropsychopharmacol. Biol. Psychiatry* **30**, 374–388 (2006).
30. Rauch, S.L. Neuroimaging and neurocircuitry models pertaining to the neurosurgical treatment of psychiatric disorders. *Neurosurg. Clin. N. Am.* **14**, 213–223 vii–viii (2003).
31. Cattaneo, E. *et al.* Loss of normal huntingtin function: new developments in Huntington's disease research. *Trends Neurosci.* **24**, 182–188 (2001).
32. Deng, H., Le, W.D., Xie, W.J. & Jankovic, J. Examination of the SLITRK1 gene in Caucasian patients with Tourette syndrome. *Acta Neurol. Scand.* **114**, 400–402 (2006).
33. Keen-Kim, D. *et al.* Overrepresentation of rare variants in a specific ethnic group may confuse interpretation of association analyses. *Hum. Mol. Genet.* **15**, 3324–3328 (2006).

ONLINE METHODS

Mice. All experiments were approved by the Animal Care and Use Committee of the Weill Cornell Medical College. We generated *Slitrk5*$^{-/-}$ mice with the previously described high-throughput VelociGene[16]. The expression pattern of *Slitrk5* was determined by the detection of β-galactosidase activity. Detailed methods are located in the **Supplementary Methods**. All experiments were performed blinded to genotype.

Tissue processing and immunostaining. We transcardially perfused mice and postfixed the brains with 4% paraformaldehyde and obtained 40-μm serial coronal frozen sections. For immunofluorescence, we stained free-floating sections with antibodies to β-galactosidase (2 μg ml^{-1}, Chemicon) and to NeuN (1 μg ml^{-1}, Chemicon) and detected with Alexa-conjugated secondary antibodies (2 μg ml^{-1}, Invitrogen). Nissl staining was performed as described previously[34]. For staining of neurons in culture, striatal neurons grown on glass coverslips (8 d *in vitro*) were fixed in 3.7% paraformaldehyde and permeabilized with 0.2% Triton X-100. We used Flag-specific antibody (1 in 1,000, Sigma) and Alexa-conjugated secondary antibodies (Invitrogen) for the detection in coimmunofluorescence experiments. We used lipofectamine (Invitrogen) to transfect striatal neurons with PSD95 fused to mCherry (a kind gift from Dr. R.H. Edwards).

Behavioral analysis and fluoxetine treatment. We performed 20-min videotaping sessions on 3-month-old mice for 2 consecutive days at 9:30, 13:30, 16:30 and 19:00. We treated the mice for 21 d with fluoxetine (Sigma) delivered in the drinking water as previously described[34]. Detailed methodology can be found in the **Supplementary Methods**.

Open-field test. The open-field test was performed as previously described[34]. Detailed methodology can be found in the **Supplementary Methods**.

Stereological volume and cell density estimations. Volume and cell density estimations were performed with the Stereoinvestigator System (Microbrightfield). After systemic random sampling, we traced brain structures using the Allen Mouse Brain Map as a reference. Striatal and total brain volumes were calculated based on traced contours by the Cavalieri estimation method. Fractionator probe was used for the stereological estimation of cell density (**Supplementary Fig. 9**). Detailed methodology can be found in the **Supplementary Methods**.

Golgi impregnation and tracing. We impregnated fresh brains in Golgi-cox using the FD Rapid GolgiStain Kit (Neurodigitech) solution for 14 d at 25 °C in the dark and then transferred them to 30% sucrose at 4 °C for 72 h. We prepared 150-μm coronal serial sections with a vibrotome; slides were soaked in 50% sucrose and air-dried for 72 h in the dark. Quantitative microscopy was performed on a Microbrightfield imaging system (Microbrightfield). Two hundred striatal neurons were chosen by systemic random sampling, and 40 'traceable' neurons for each genotype were reconstructed three dimensionally with the Neurolucida system. The morphological traits of cells were analyzed with Neuroexplorer.

Electrophysiology. We killed 4-month-old mice by pentobarbital anesthesia to obtain corticostriatal slices for electrophysiological recordings. Coronal brain slices (400 μm) were made on a vibrotome (Campden Instruments) and submerged in artificial cerebrospinal fluid in a brain-slice keeper (Scientific Systems Design) for 90 min at 25 °C and gassed with 95% O_2, 5% CO_2 before transfer to the recording chamber[35]. The artificial cerebrospinal fluid contained 118 mM NaCl, 2.5 mM KCl, 10 mM glucose, 1 mM NaH_2PO_4, 3 mM $CaCl_2$, 2 mM $MgCl_2$ and 25 mM $NaHCO_3$. 100 μM picrotoxin was included in the recording solution. Recording electrodes were filled with 2 M NaCl solution, and population spikes were recorded from the striatum with the IE-210 amplifier (Warner Instruments) using Digidata 1440A and pClamp 10 software (Molecular Devices) at 32 °C. For synaptic stimulation, we placed bipolar electrodes in the white matter between the cortex and the striatum to activate corticostriatal fibers[35]. Population spike amplitude was calculated by the mean of the amplitude from the first peak positivity to the peak negativity of the population spike and the amplitude of the peak negativity of the population spike to the second peak positivity[36,37]. The presynaptic fiber volley amplitude was measured as a difference between the initial positive and the following negative peak. Three consecutive responses were averaged for measuring the spike and fiber volley amplitude. Paired-pulse responses were evoked at interstimulus intervals of 20, 40, 80, 120 and 200 ms using a stimulation intensity of 0.9 mA. Paired-pulse ratio is defined as the ratio of second population spike amplitude to the first population spike amplitude. Population spike amplitudes were analyzed by Clampfit software (Molecular Devices).

Neuronal culture. Rat primary striatal neuron cultures were prepared as described previously, with a few modifications[38]. Detailed methodology can be found in the **Supplementary Methods**.

Immunoblotting. Immunoblotting was performed as previously described[38] with antibodies to the following proteins: NR2A (Covance), NR2B (Invitrogen), GluR1, GluR2, NR1, PSD95 (all Chemicon) and actin (Santa Cruz). Detailed methodology can be found in the **Supplementary Methods**.

Statistical analyses. Data are shown as means ± s.e.m. We used Student's *t* test to calculate statistical significance between group differences. Significance was set at $P < 0.05$. We used two-way ANOVA with repeated measures to analyze behavioral performance in the rotarod test and electrophysiological studies. We performed data analysis using Prism 4.0 (GraphPad software) for neuron tracing.

34. Chen, Z.Y. *et al.* Genetic variant BDNF (Val66Met) polymorphism alters anxiety-related behavior. *Science* **314**, 140–143 (2006).
35. Picconi, B. *et al.* Loss of bidirectional striatal synaptic plasticity in l-DOPA–induced dyskinesia. *Nat. Neurosci.* **6**, 501–506 (2003).
36. Lovinger, D.M., Tyler, E.C. & Merritt, A. Short- and long-term synaptic depression in rat neostriatum. *J. Neurophysiol.* **70**, 1937–1949 (1993).
37. Alger, B.E. & Teyler, T.J. Long-term and short-term plasticity in the CA1, CA3 and dentate regions of the rat hippocampal slice. *Brain Res.* **110**, 463–480 (1976).
38. Pereira, D.B. & Chao, M.V. The tyrosine kinase Fyn determines the localization of TrkB receptors in lipid rafts. *J. Neurosci.* **27**, 4859–4869 (2007).

doi:10.1038/nm.2125